Estimation of rock fracture properties from thermal variations of the groundwater discharge into a tunnel

Milan Hokr
Milan.hokr@tul.cz
Aleš Balvín
Ales.balvin@tul.cz
Petr Rálek
Petr.ralek@tul.cz
Technical University of Liberec, Studentská 2, Liberec, 46117 Czech Republic

ABSTRACT: We study the coupled water flow and heat transport (conduction and advection) in a neighborhood of a tunnel in fractured granite (in up to 150 m depth in Jizera mountains, Czech Republic). The temperature in the tunnel changes quasi-periodically in the annual cycle, affecting the rock temperature and the discharge water temperature. This is captured by an axisymmetric model of a fracture perpendicular to the tunnel (with advective heat transport) and a surrounding matrix block with conduction only. The model is successfully fit to measurement and some of the parameters or features not specified from the measurement and from the hydraulic model can be estimated. On the other hand, due to model simplification, it is sensitive on an artificial parameter which has not a realistic counterpart (a gap in the boundary condition).

INTRODUCTION

Modelling of thermal phenomena in groundwater is of larger interest e.g. in the geothermal applications or the safety analysis of the spent nuclear fuel repository. As a coupled problem of the water flow and the heat transport, the solution and interpreting the model and the parameters with respect to the measurement becomes more complex.
There are studies in groundwater considering temperature as a kind of tracer. It typically considers larger scale – e.g. between infiltration and discharge, taking into account the altitude and the depth (e.g. Maréchal and Perrochet, 2001). It is not typical to observe thermal field in a scale of tenths of meters to meters in field conditions, with feasible measuring sensor positioning for obtaining sufficient modelling data. Example of model with network of fractures is by Birkholzer et al. The feature is then the inhomogeneity – instead of a quasi-uniform flow and a local thermal equilibrium in porous (or dual-porosity) medium, we are interested in the interaction between a single fracture and the surrounding compact rock blocks, with captured temperature distribution perpendicular to the fractures.
We continue our previous work on model and field data comparison, presented in conferences (Hokr and Straka, 2014), in particular by extending the data sequence length to get better validation and by evaluating additional parameter sensitivity.

SITE CHARACTERISATION AND OBSERVED DATA

The studied problem comes from the water supply tunnel Bedrichov, in the granite massif of the Jizera mountains in the north of the Czech Republic (Fig. 1 left). It is a part of a multidisciplinary geoscientific project, started in 2003 by the Czech Geological Survey and currently managed by the Technical University of Liberec (TUL) (Klomínský and Woller, 2010, Hokr et al 2014). The tunnel is 2600 m long and reaches the maximum depth of approximately 140 m. The tunnel was constructed between the 70s and 80s for conducting water from a reservoir to a processing plant, by means of a pipe of 80 cm diameter. The research is motivated by observing the physical phenomena in rock conditions, considered as analogous to the spent nuclear fuel repository (except the depth). This work is related to monitoring of groundwater discharge into the tunnel and of rock and water temperatures.

The main features of the hydrogeological conditions are the shallow permeable zone, which is 20-30 m deep (based on the tunnel observations and surface boreholes) and the deeper hard rock with systems of fractures and several more important sub-vertical faults. The water inflow is the evidence of this model, with dominant contribution in the shallow parts (moreover influenced by the water reservoir) and several places with smaller observable inflow in the deeper part (Fig. 1 right). The temperature in the tunnel is controlled by the water transporting pipe and it is basically seasonally influenced but with a lot of irregularities (visible below, as a part of the results presentation). Consequently, the variations spread into the rock with decreasing amplitude and peak delays. In a long time scale, it is assumed that the tunnel cools the rock around it, but because of the year-to-year differences, it is difficult to interpret the average temperatures in the tunnel and deeper in the rock. The temperatures of the groundwater seeping into the tunnel have also temporal variations corresponding to the air and rock temperatures, but these are of decreasing range with increasing flow rate, which is interpreted by the conceptual model of a local non-equilibrium between a water bearing structure and compact rock blocks around (Fig. 2 left).

Measured data

The hydraulic measurement is operated by the Technical University of Liberec (a team of the authors – Rálek and Hokr, 2013) and the rock temperatures are monitored by the Geophysical Institute of the Academy of Sciences of the Czech Republic (GFU). From more than ten points of the inflow rate monitoring, we select two with the longest data sequence and representative conditions (Tab. 1): The first at 225 m chainage, from a single fracture in hard rock, quite close from the shallow permeable zone above, the flow rate approximately 2 ml/s. The second at 1727 m chainage, from a hose through concrete cover at an intersection of the tunnel with a larger sub-vertical fault, the captured flow rate approximately 10 ml but with large distributed water discharge around the sampled one.

The rock temperatures are measured in boreholes perpendicular to the tunnel, in profiles of several sensors up to the 3.6 m depth (Šafanda and Dědeček, 2014). The data from the position 248 m are used for the study, assuming the temperature along the tunnel is approximately uniform (due to large capacity of the water pipe, and confirmed by the sensors). On the other hand, due to air convection in the tunnel, it is some uncertainty on the rock surface temperature along the tunnel circumference. The seasonal variations are between 3 and 12 °C in the air and between 4 and 9 °C in shallow below the surface of the rock. The amplitude decreases to below one degree in the 3 m depth, similar to the water temperature variations of stronger inflow points.

Figure 1: Position of the studied site in the left, photos inside the tunnel in the bored part with very little inflow on bare rock and in the blasted part with inflow through a concrete-covered fault intersection.

MODEL DESCRIPTION

Concept and geometry

The model concept and basic features are presented in Fig. 2. We aim to capture the heat conduction perpendicular to the tunnel, advection by the water in a fracture, and the heat conduction perpendicular to the fracture. We make several assumptions to keep the model simple. The first is the axial symmetry – it means that the fracture is perpendicular to the tunnel axis and the water flow is uniform in the fracture plane (which is contrary to observation, but anyway, we do not have any available data to describe the flow more precisely in the model). The second is a discontinuous transition between the water permeable layer and the surrounding compact rock. Next, we do not represent the larger-scale thermal inhomogeneity (advection effect on the geothermic gradient) and assume perfect thermal equilibrium far enough from the tunnel (a basic fact of the average thermal gradient around the tunnel is detected by the model calibration – below). Also we define a spatially-uniform time-variable temperature of the rock surface (tunnel wall), based on a single point measurement, which simplifies the real convective air-rock heat exchange, resulting to potentially non-uniform rock surface temperature depending e.g. on a distance from the fracture. This is commented in the results as the sensitivity on the temperature boundary position (gap size).

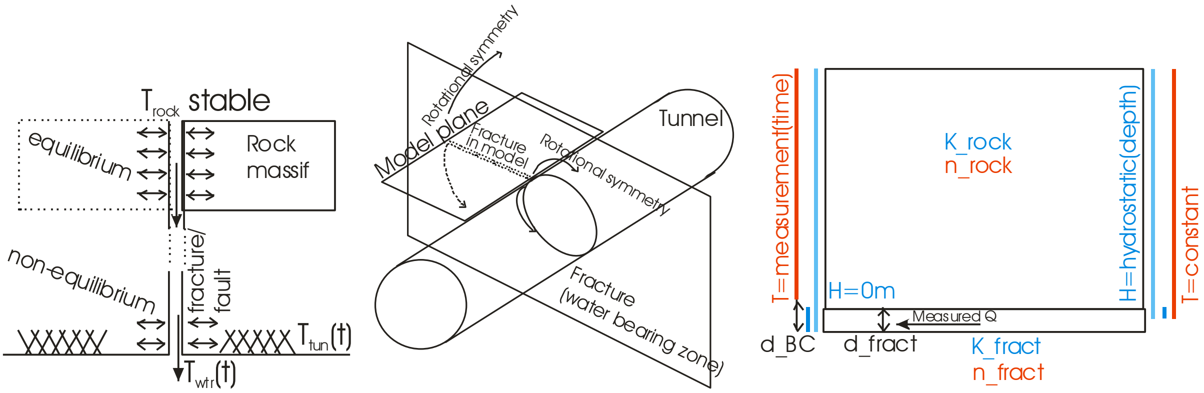

Figure 2: From the left – conceptual model of thermal water-rock interaction, approximation of the field conditions by the axisymmetric model, and position of parameters and boundary conditions in the model plane (the rotational axis is the vertical). The values differ by model variants.

The dimensions of the model are 8 m in the radial direction and 6 m in the axial direction (one symmetric half). We consider several variants of the fracture representation – the mesh is prepared with “layers” allowing to define the permeable zone of thicknesses of 0.04 m, 0.14 m, 0.74 m, and 1.34 m (meaning in the “reality” of both symmetric parts included – Fig. 3). The tunnel wall edge is 1.75 m from the axis, corresponding to 3.5 m tunnel diameter. We also tested the 1D discrete feature for the fracture representation with similar results, but this is not presented in the paper.

Hydraulic data

The hydraulic boundary conditions represent the gradient controlled by the tunnel drainage – zero pressure in the tunnel and a pressure in the 8 m depth derived from the analytical solution of radial flow with outer boundary in the distance equal to the depth below the surface, considering hydrostatic pressure of this depth (Tab. 1, third column). The boundary conditions are prescribed either along the whole edge, or only at the permeable zone (Fig. 2 right), with negligible effect on the results. The only prescribed parameter is the hydraulic conductivity which is negligible in the rock domain and the value for the fracture depends on the thickness, to keep the transmissivity and to fit the observed flow rate (Tab. 1). There are two options how to interpret the measurement for the model – the measured inflow is typically concentrated to a part of the tunnel circumference, so we need to consider a larger total inflow in the axisymmetric model, to “project” the water-bearing part into the remaining circumference (here e.g. a 2π factor). We consider the hydraulic model as steady-state, which is appropriate for the observed flow rate variations within 10-20 %, with small effect on the temperatures.

Thermal data

The thermal boundaries are prescribed temperatures on the edge representing the tunnel surface and on the parallel edge representing the rock far from the tunnel in equilibrium. The former is defined by the measurement data sequence, while the latter is approximated by a constant. As the first estimate, we use the average of the tunnel temperature during the full data period (6.67 °C), which was finally revised to a little larger value of 7 °C. The parameters are listed in Tab. 2. The heat conductivity and capacity is well based on both laboratory samples and in-situ data (rock conduction model calibration), while the others are rough estimates based on general literature values and recommendations. The effect of the porosity was negligible (i.e. only total heat flow rate is important, not the actual transport velocity), the effect of the dispersivities was little larger. We do not mind the initial condition (which cannot be well supported by data) – it was defined constant at the beginning, and then the end of previous simulations was used for the next, considering the first year as a “warm-up” (before the considered data for the model-measurement comparison and other evaluation). For simpler presentation, we consider the time scale as numbers in years. The zero point correspond to 1st Jan 2010, the data end in the second half of 2015 – so the 5 years are simulated, from them about 3.75 year is available for evaluation.

A special comment is on the position of the tunnel temperature boundary. To evaluate the discharge water temperature by the node observation point, we need to exclude a part of the edge across the fracture from the boundary condition – this is represented by the distance d_BC in Fig. 1, keeping some gap between the fracture and the temperature boundary. In the previous studies, we evaluated the effect of the fracture thickness on the intensity of the fracture-rock interaction. We detected now that most of this effect results from the position of the boundary condition (d_BC), rather than the fracture thickness itself (see results below). In the models fitting the data, the distance d_BC is typically twice the d_fract (keeping a part of the rock not interacting with the tunnel air).

	flow rate [ml/s] (full circ.)	depth [m]	pressure dif [m]	fracture transmissivity (K*d_frac) [m²/s]
1727m measurement represents 1rad	62.8	90	39	4.402E-07
1727m meas. represents full circumference	10	90	39	7.010E-08
225m measurement represents 1rad	12.57	42	22.7	1.514E-07
225m meas. represents full circumference	2	42	22.7	2.409E-08

Table 1: Variants of hydraulic conditions and parameters corresponding to observed inflow points and different meaning of the measurements.

	rock matrix	fracture
hydraulic conductivity [m/s]	3.50E-10	Tab. 1
porosity	0.01	0.3
solid heat conductivity [W/m/K]	3	3
solid vol. heat capacity [J/m³/K]	2.50E+06	2.50E+06
longitudinal dispersivity [m]	2	2
transversal dispersivity [m]	0.2	0.2

Table 2: List of parameters for the two model subdomains. There are several variants of the fracture hydraulic conductivity depending on the model variant (flow rate and fracture width).

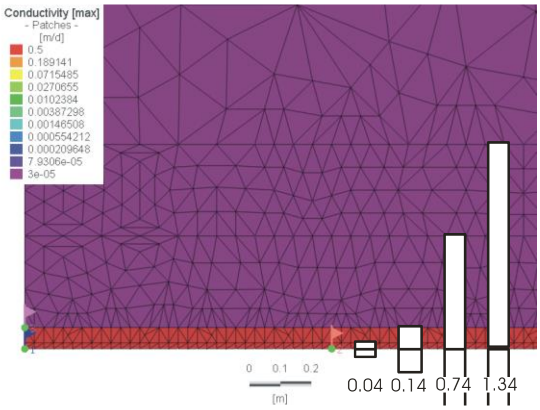

Figure 3: Fragment of the model mesh in the bottom left corner (fracture discharge to the tunnel) where the four variants of the fracture domain thickness are illustrated with the attached values in meters (both symmetric parts).

RESULTS

We followed several aims in the evaluation. Basically, the conceptual model is verified by a comparison with the measured temperatures of both the water and the rock. Then, the model fitting is used for a calibration of the data, in particular the fracture characteristics additional to those resulting from the hydraulic model. In the previous studies, we interpreted the hydraulic parameters of the fractures intersecting the tunnel by larger-scale models (Hokr et al. 2014). The calibrated value is the transmissivity, so that we cannot distinguish the volume of rock in contact with water. Besides this, the total volume of mobile water (or the porosity) can be estimated from natural tracers, the transport velocity derived from the residence time. Additionally, sensitivity of the model on various parameters is evaluated without resulting to a particular calibrated parameter value.

Rock conduction evaluation

We start with evaluation of the rock conduction model – the reference conditions for including the effect of advection in the fracture, with available measured data. The corresponding observation points are in the opposite part of the model than the fracture (no.4 to 7 in Fig. 7). The results for three selected depths are in Fig. 4. We compare two variants of the boundary temperature against the measurement. We see that the increased temperature over the tunnel average clearly improves the fit, the deeper the larger effect of the change. Besides the correct heat conduction parameters of the model, we also verified the appropriate distance from the fracture with disappearing effect of the advection on the surrounding rock.

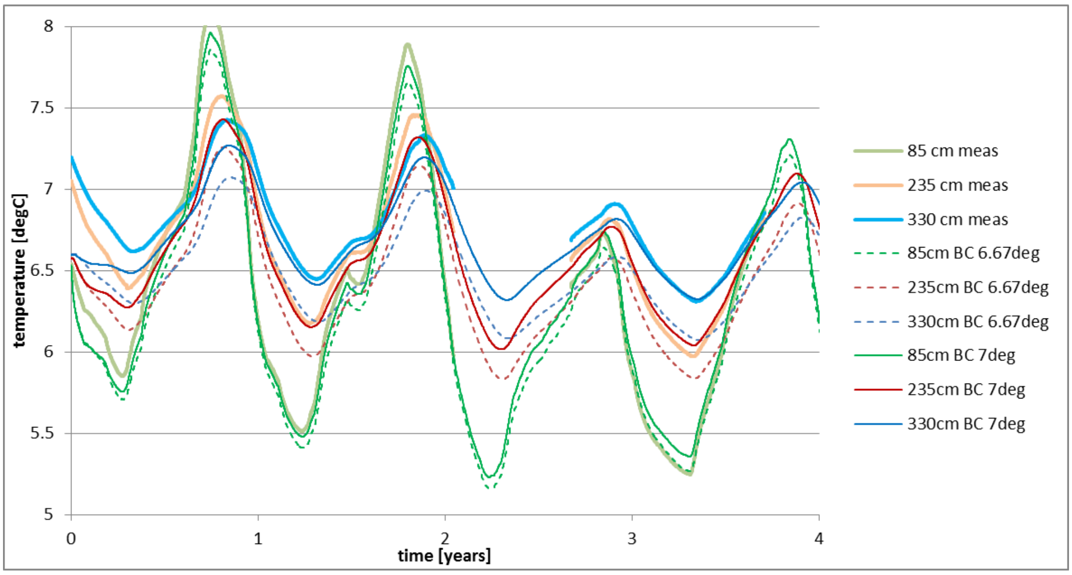

Figure 4: Time evolution of rock temperatures in various depth, two variants of model with different rock boundary temperature.

Discharge water temperature evaluation

We evaluate two measurement points with contrasting properties – one is the larger flow rate at 1727 m chainage with smaller water-rock equilibration and smaller temperature variations, second the smaller rate at 225 m chainage with larger water-rock equilibration and larger temperature variations. The models are fitted to data by setting the three most-sensitivity parameters: the total flow rate (full model circumference with respect to the measured flow position), distance of the temperature boundary from the fracture (a gap, related to the fracture "width"), and the boundary temperature on the edge inside the rock.

To fit the 1727 m data (Fig. 5), the larger flow must be set, i.e. approx. 60 ml/s total from around the tunnel, correcting the incomplete capture of inflow with 10 ml/s rate (Tab. 1), which is well acceptable considering the visual observation. The sensitivity on the fracture width and the boundary distance is commented below. For the fit, the choice of the smallest fracture width with the largest boundary distance was necessary (smallest interaction). This is contrary to the observation of the wider water-permeable zone. Finally, it was necessary to use the increased equilibrium temperature on the boundary inside the rock, consistently with the comparison of the rock temperatures in the conduction-only part of the model domain. The contrast between the very good fit of variations in the period 3-5 years, to the smaller measurement variations in the period 1-3 years can be explained by the recorded change of the flow rate in the measured hose after some manipulation with the equipment in the respective period (2012).

The variations of the 225 m water temperature are close to the equilibrium with the rock which is visible from joint presentation of these data and the model in Fig. 6. Here, the flow rate variant with the measured value spread around the full circumference is used (the smaller rate from the choice). The sensitivity on the boundary temperature inside the rock is obviously smaller. The effect of the gap in the tunnel temperature boundary is still significant, but cannot be uniquely fit to the data due to large noise in the measurement of a comparable magnitude.

The two cases are also compared by the spatial temperature distribution pattern in Fig. 7 – we can see a gradient similar in the rock matrix and the fracture parts for the smaller flow rate and a significant contribution of advection for the larger flow rate.

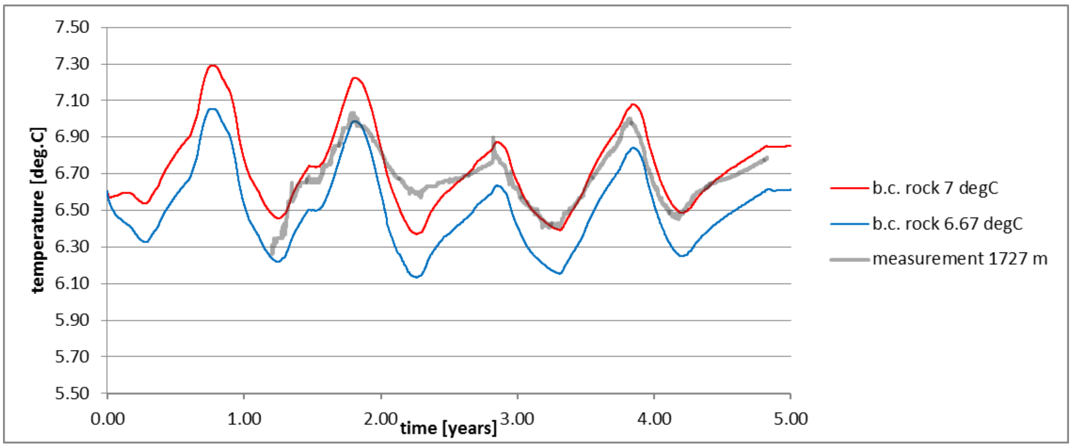

Figure 5: Time evolution of temperature of the water discharge, for the 1727 m measurement point conditions, two model variants for different internal rock boundary temperature.

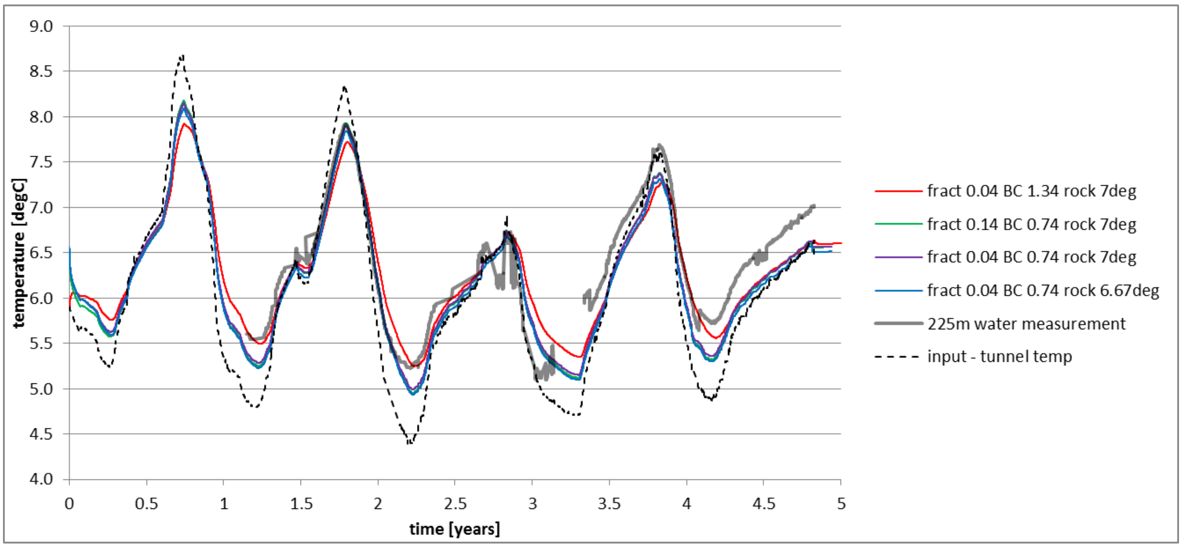

Figure 6: Time evolution of temperature of the water discharge, for the 225 m measurement point conditions, several model variants (fracture width and the b.c. distance in meters) and the tunnel rock surface temperature variations are presented.

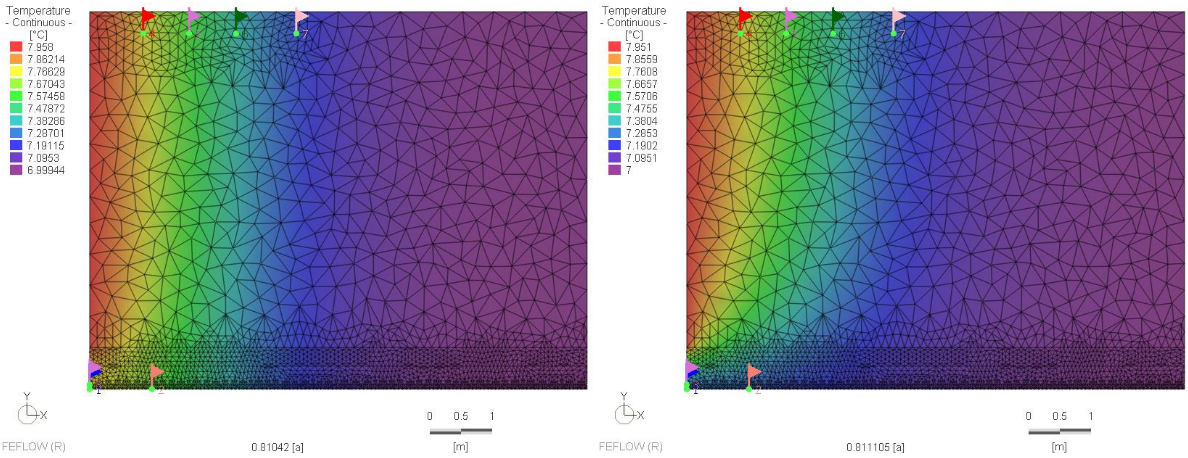

Figure 7: Spatial temperature distribution for the two different hydraulic conditions – more uniform field for the smaller flow rate in the left and more advection-influenced field for the larger flow rate in the right (the left side is the tunnel wall, the bottom side is the fracture).

Parameter sensitivity

There were several parameters which were uncertain and/or not supported by available data (commented above) – the porosity, the dispersivity, the permeable zone (fracture) width, the distance of the temperature boundary from the fracture. The parameters with a smaller effect are not presented here due to limited space. The larger dispersivity contributes to the larger interaction. In Fig. 8, the effect of the fracture width and the thermal boundary gap commented above is presented. The difference between the two distances corresponds to the gap without any prescribed boundary. The effect of the fracture width is significant typically indirectly by changing the gap. To evaluate the effect of the fracture width appropriately in the calibration above, we consider e.g. a constant ratio between the fracture width and the gap in the boundary.

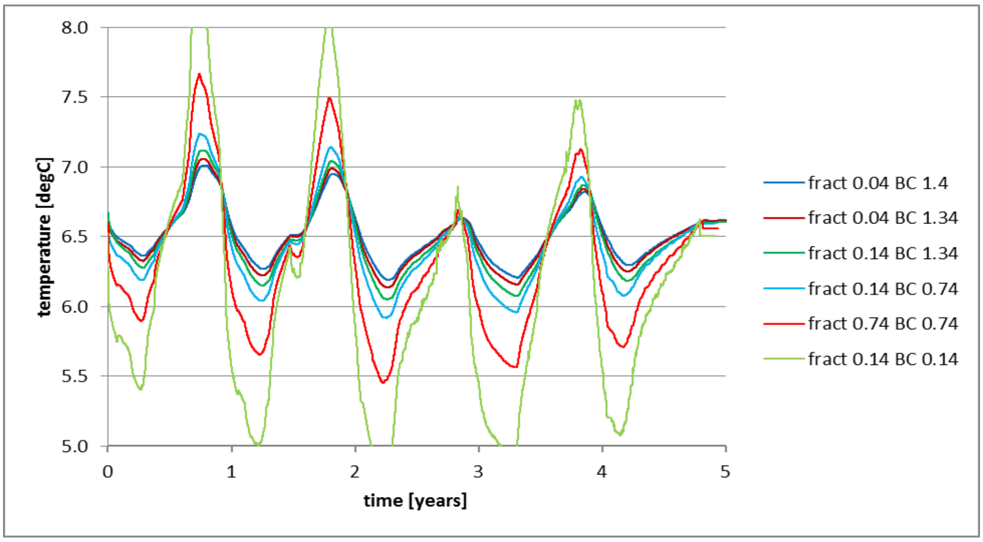

Figure 8: Comparison of model water temperature time evolution for several parameter combinations – the fracture width (meters) and the distance of the temperature boundary from the fracture symmetry plane (meters).

CONCLUSION

The presented model confirms a general conceptual model of the coupled advection in a fracture and conduction in rock matrix. Previous work of authors is extended to several years data sequence, making the comparison more reliable. On the other hand, the previous conclusions on the estimated water-rock contact zone thickness were corrected due to significant effect of the artificially chosen gap between the fracture position and the prescribed temperature position at the tunnel wall.

For the future, the model problem is considered for verification of the Flow123D software developed at TUL. Also, work on a larger scale model of the advection effect on the temperature field between the tunnel and the surface is in progress, possibly providing more precise temperature value at the rock boundary.

REFERENCES

Birkholzer, J.T , Zhang, Y.: The impact of fracture-matrix interaction on thermal-hydrological conditions in heated fractured rock. – Vadose Zone Journal 5 (2006), pp. 657-672.

Hokr M., T. Straka, and VITA project team, Modelling of Rock-Water Thermal Interaction in Different Scales, PROCEEDINGS of Thirty-Ninth Workshop on Geothermal Reservoir Engineering, Stanford University, 2014, 8pp.

Hokr, M., A. Balvín, I. Škarydová, P.Rálek, Tunnel inflow in granite – fitting the field observations with hybrid model of discrete fractures and continuum. In Sharp and Troeger, ed. Fractured Rock Hydrogeology. IAH - Selected Papers on Hydrogeology: 2014, pp. 241–256.

Klomínský, J. ,Woller, F. (eds.), Geological studies in the Bedrichov water supply tunnel. RAWRA Technical Report 02/2010, 103 p. Czech Geol. Survey, Prague. ISBN 978-80-7075-760-4.

Maréchal, J.C. and Perrochet P., Theoretical relation between water flow rate in a vertical fracture and rock temperature in the surrounding massif. Earth and Planetary Science Letters 2001, pp.213–219.

Rálek P., Hokr M.: Methods of Water Inflow Measurement in the Bedřichov Tunnel. EGRSE. Explor. Geophys., Remote Sens. Environment, 2(2013), pp.30–39.

Šafanda J., Dědeček P., Temperature monitoring, In Hokr (ed.) Tunel 2011 Final report, SURAO, 2014 (not published).

ACKNOWLEDGEMENTS

This work has been supported by TAČR, project code TA04020506 and by SÚRAO, contract code SO2011-017. The results were also obtained through the financial support of the Ministry of Education, Youth and Sports from the project LO1201 in the framework of the targeted support of the "National Programme for Sustainability I". The authors thank to the water management company (SČVK a.s.) operating the tunnel, for allowing the access for the monitoring.